12-6-2021

Surface Pressure Measurements in Translating Tornado-Like Vortices

Aya Kassab

Chowdhury Jubaye

Arash Ashraf

Horia Hangan

Surface Pressure Measurements in Translating Tornado-Like Vortices

Aya Kassab*[1], Chowdhury Jubayer[1], Arash Ashrafi[1] and Horia Hangan [1]

[1] *WindEEE Research Institute, Western University, 2535 Advanced Ave., London, ON, Canada, N6M 0E2*

(Received keep as blank , Revised keep as blank , Accepted keep as blank)

Abstract. High spatial and temporal surface pressure measurements were carried out in the state-of-the-art tornado simulator, the Wind Engineering, Energy and Environment (WindEEE) Dome, to explore the characteristics of stationary and translating tornado-like vortices (TLV) for a wide range of swirl ratios (S=0.21 to 1.03). The translational speed of the TLV and the surface roughness were varied to examine their effects on tornado ground pressures, wandering, and vortex structure.

It was found that wandering is more pronounced at low swirl ratios and has a substantial effect on the peak pressure magnitude for stationary TLV (error percentage ≤ 35%). A new method for removing wandering was proposed which is applicable for a wide range of swirl ratios. For translating TLV, the near-surface part lagged behind the top of the vortex, resulting in a tilt of the tornado vertical axis at higher translating speeds. Also, a veering motion of the tornado base towards the left of the direction of the translation was observed. Wandering was less pronounced for higher translation speeds. Increasing the surface roughness caused an analogous effect as lowering the swirl ratio.

Keywords: Tornado-like vortices, Surface pressure, Swirl ratio, Roughness, Translation speed, Wandering, Tilting, Veering

1. Introduction and background

Tornadoes are considered as one of the most violent and destructive weather phenomena. Nearly over 1,000 tornadoes are reported annually in the United States and their damages can exceed over one billion dollars (NOAA, 2012). One of the deadliest tornadoes on record was the Joplin tornado on May 22, 2011, an EF–5 rated tornado which caused 158 fatalities, more than 1,000 injuries, and left nearly 7,500 residential structures partially or totally collapsed (NWS, 2011). This demonstrates the severity of tornadoes and the vulnerability of buildings under these fierce storms. The destruction of structures due to tornadic hits is associated with exceeding the permissible design wind loads in building codes, e.g., ASCE 7-16 (ASCE/SEI, 2016) or NBCC 2015 (NRCC, 2015) which rely solely on the atmospheric boundary layer (ABL) flow-fields in calculating pressure coefficients.

*Corresponding author, Ph.D., E-mail: akassab@uwo.ca

This destruction can be minimized substantially by designing the buildings to withstand tornadoes up to EF-2 rated tornadoes which occupy 95% of tornado hits in the United States according to NOAA. In order to achieve this, a rigorous analysis of the tornado induced pressures and the resulting loading on structures is needed. A key component in this analysis is the characterization of tornadic ground pressures for various tornado intensities, translational speeds, and surface roughness. While full scale, numerical and experimental studies of tornado induced pressures have been performed (e.g. Lee and Wurman 2005; Natarajan and Hangan 2012; Mishra *et al.* 2005), there are gaps in understanding the effects of translation and roughness of TLV as well as their relation to tornado surface trajectories and wandering.

Owing to the difficulty to predict tornado onset, their probable trajectory, and the adversity of implementing measuring instruments of tornado flow-field near the ground, very few field tornado measurements have been reported in the literature. Field tornado measurements have seen developments since their earliest attempts utilizing weather stations and barometers (Tepper and Eggert 1956; Fujita 1958). Doppler radars were later employed to explore tornado characteristics (Wurman *et al.* 1996; Wurman and Gill 2000; Wurman 2002; Bluestein *et al.* 2004; Lee and Wurman 2005; Alexander and Wurman 2005a, 2005b; Wakimoto *et al.* 2011; Wakimoto *et al.* 2012). By 1995, the Doppler On Wheels (DOW) was introduced which permitted a safer environment for scientists to record data (Wurman *et al.* 1997). Moreover, very few studies about ground pressure measurements were accomplished due to the difficulty and challenges in setting up the instruments in the unpredictable path of the tornado (Lee and Samaras 2004; Wurman and Samaras 2004; Karstens *et al.* 2010). Hardened In-Situ Tornado Pressure Recorder (HITPR) probes and mobile mesonet were utilized in those studies to obtain pressure and velocity measurements.

Furthermore, the signature of the tornado on the ground was reported in most of the field studies utilizing satellite images and tornado damage on the ground, where the tornado path in most of the cases veers in a curved path rather than a straight-line path (Wakimoto *et al.* 2003; Lemon and Umscheid 2008; Karstens *et al.* 2010; Wurman and Gill 2010). Lee *et al.* (2004) deployed three conical-shaped HITPR probes in the path of a F-4 tornado in Manchester, SD to measure the tornado loading on the ground, temperature, wind speed, and humidity. They deduced that the tornado path is curved rather than a straight line and that the pressure deficit is not perfectly symmetrical. Moreover, they compared the pressure deficit profile with two analytical models, Rankine and Burgers-Rott models, where the latter proved to provide a better agreement. Karstens *et al.* (2010) utilized HITPR, mobile mesonets, and video probes in nine tornado events since 2002 to reveal the near-ground characteristics of tornadoes in terms of pressure deficits, and in some cases velocity profiles as well. They revealed the structure of the nine tornado volumes and found that they are ranging between single-celled, double-celled, and multiple-celled tornadoes. They also calculated the translation speed of all nine events and analyzed the tornado path using visualization, video probes, and radar images. Albeit the reliability and robustness of field tornado measurements in characterizing tornado flow-field, the measurements are confined to higher heights above most of the vital structures, particularly low-rise buildings. This is because the radar should be positioned distantly above all the obstacles to provide reliable data. These challenges associated with the field measurements lead to the rising of experimental work using tornado vortex chambers and numerical simulations in parallel with the hard-to-accomplish field studies.

Numerical simulations have been broadly used by many researchers due to their adjustability and lower cost compared to experimental and field studies and have been improved through the years (e.g. Lewellen *et al.* 1997; Nolan and Farrell 1999; Nolan 2005; Ishihara *et al.* 2011; Natarajan and Hangan 2012; Liu and Ishihara 2015, 2016; Nasir and Bitsuamlak 2016; Nolan *et al.* 2017; Gairola

and Bitsuamlak 2019). Numerical studies covered different topics exploring the stationary and translating tornadic flow field, examining tornado-structure interaction, and tornadic post-damage studies. Tornado translation was found to create secondary vortices (e.g. Diamond and Wilkins 1984). Also, the effect of roughness was investigated in some studies that provided contradicting results regarding the vortex diameter either decreasing with increasing roughness (Diamond and Wilkins 1984; Zhang and Sarkar 2008) or increasing with increasing roughness (Dessens 1972; Leslie 1977; and Natarajan and Hangan 2012). These contradicting results are indicative of the need to validate numerical simulations against laboratory or where possible, field measurements.

Laboratory simulations of TLVs have been started since the early seventies when Ward (1972) built the first tornado simulator. Ward (1972) explored tornado features by comparing laboratory results with field tornadoes and found that the radial momentum flux is a vital factor in producing tornadoes and that the vortex is very sensitive to the geometrical parameters of the simulator. The simulator's main drawbacks were its limited access to the vortex chamber due to its small size which did not allow adding appropriate-sized building models for studying tornado-structure interaction and that it did not support tornado translation. Subsequently, several Tornado Vortex Chambers (TVC's) have been constructed to identify and examine the aerodynamic behavior of tornado-like flows (Church *et al.* 1979; Mishra *et al.* 2005; Haan *et al.* 2008; Hangan 2014). Although laboratory simulation was adopted by many researchers who performed vast advancements for better characterization of tornado flow-field, it has some restrains. Most of the tornado simulators lack the ability to create the translational motion of simulated tornadoes (Ward 1972; Church *et al.* 1979; Mishra *et al.* 2005; Hashemi Tari *et al.*, 2010). Moreover, the limited size of most of the tornado simulators confines the ongoing research as it does not provide the adequate resolution for measuring the tornadic loads on buildings (Ward, 1972; Church *et al.*, 1979; Snow, 1982). Posterior efforts were exerted to investigate the pressure loadings on different structures (e.g. Mishra *et al.* 2008b; Haan *et al.* 2010; Kikitsu and Sarkar 2011; Hu *et al.* 2011; Thampi *et al.* 2011; Rajasekharan *et al.* 2013; Case *et al.* 2014). However, there are some uncertainties about the geometric and the velocity scaling of most simulators which have a direct effect on the aerodynamic loading (Baker and Sterling, 2019).

Tari *et al.* (2010) conducted experiments in a small tornado vortex simulator (TVS) at Western University, Canada to investigate the swirl ratio effects on tornadic flow characteristics. They concluded that the core radius, the tangential, and radial velocities rise with increasing swirl ratio. In addition, the vortex touchdown stage recorded the highest turbulent kinetic energy. Zhang and Sarkar (2012) investigated the near-ground flow-field of stationary TLVs using PIV system. They found that wandering affected the results, particularly for lower swirl ratios and that the intensified mean flow in collaboration with high turbulence near the ground and large pressure deficit would have a prominent role in buildings' destruction. Nevertheless, this investigation was circumscribed to lower swirl ratios ($S < 0.3$), and the radial Reynolds number range was debatable. Refan *et al.* (2014) utilized Particle Image Velocimetry (PIV) in the Model WindEEE Dome (MWD) to investigate the TLV structure and compared the results with full-scale data utilizing the Ground-Based Velocity Track Display (GBVTD) method. They deduced the geometric scale and the equivalent swirl ratio of tornadoes in MWD and found that the MWD is capable of reproducing tornadoes equivalent to EF0 to EF3 tornadoes in field tornadoes. Tang *et al.* (2018) carried out experiments in the VorTECH tornado simulator at Texas Tech University. They studied the mean and turbulent characteristics of stationary TLVs using cobra probes and omniprobes for velocity measurements and static pressure taps on the ground for surface loading calculations. It was revealed that the fluctuating pressure widely contributed to the tornado loading and that the pressure deficit

has a good agreement with field tornadoes. Refan and Hangan (2018) explored the characteristics of stationary TLVs close to the ground over a broad range of swirl ratios using Particle Image Velocimetry (PIV) and surface pressure measurements. They deduced that wandering behavior is more pronounced at low swirl ratios and that the tornadic near-surface pressures become independent of the radial Reynolds number for $Re > 4.5 \times 10^4$.

All the efforts in examining the near-surface of TLVs have been concentrated on stationary tornadoes (Tari *et al.* 2010; Zhang and Sarkar 2012; Refan *et al.* 2014; Tang et al 2018; Refan and Hangan 2018). Hence, studying the characteristics of translating TLVs close to the ground, where the majority of structures lie, is crucial as this represents the actual behavior of real tornadoes.

In real tornadoes, the ratio between the translation velocity and the maximum tangential velocity varies in the range of 0.03 to 5 (Lombardo *et al.* 2015; Refan *et al.* 2017; Rhee and Lombardo 2018). The lack of the ability to produce translation in most of the tornado simulators resulted in few experimental studies about translating tornadoes at relatively reduced translational speeds (e.g., Haan *et al.* 2010; Sengupta *et al.* 2006, 2008; Wang *et al.* 2016). Haan *et al.* (2010) studied experimentally the effect of translating tornadic flow ($v_{translating} \leq 0.61$) on a one-story, gable-roofed building and compared it with ABL flow. They reported that translation resulted in an inclination of the vortex axis towards translation direction. However, they did not explain this phenomenon in detail. Sengupta *et al.* (2008) explored the difference between simulating stationary and translating TLVs utilizing LES on a cubic building and compared it to experimental results. They deduced that tornadic loading of F2 intensity or higher exceeded the ASCE 7-05. Most of the translating tornado studies were focused on the loading on the buildings without delving into the characteristics of the translating tornado structure near the ground. Hence, more detailed research needs to be performed to understand the characteristics of the translating tornadoes near the surface. This will provide a better understanding of the tornadic hit's outcomes in this critical region where most of the structures exist and will lead to building more tornado-resilient communities.

Although reproducing tornadoes in tornado simulators proved to be a robust method, the resulting tornadic swirl is affected by the wandering behavior of the vortex (Baker 1981; Snow and Lund 1997; Zhang and Sarkar 2012; Ashton et al 2019; Refan and Hangan 2018; Karami *et al.* 2019). Ashton *et al.* (2019) explored the wandering behavior of TLVs in tornado simulators using the data obtained from the Model WindEEE Dome (MWD). It was concluded that the extent of wandering could produce an error as high as 17%. The necessity of removing the wandering effect from the time-averaged velocity field was emphasized and two techniques were proposed to remove the wandering effect; one, re-centering the vortex by detecting the vortex center, and two, using the deconvolution method. The first method was reported to provide more rigorous results.

Most of the previous experimental studies were performed over smooth ground. Few studies adopted rough surfaces that may represent different exposures (e.g. Dessens 1972; Zhang and Sarkar 2008; Matsui and Tamura 2009; Fleming *et al.* 2013; Wang *et al.* 2017). Moreover, numerical simulations of the effect of ground roughness on tornado structure were performed (Natarajan and Hangan 2012; Liu and Ishihara 2016). Wang *et al.* (2017) found that the radial and vertical velocity fluctuations in tornadic flow are influenced by surface roughness and that introducing roughness resulted in transitioning to a lower swirl ratio. Generally, previous studies revealed that increasing roughness has a similar effect to decreasing the swirl ratio on the mean flow-field, unlike few studies that showed the reverse effect (e.g. Fleming *et al.* 2013). Despite all the efforts in the literature, a lack of a rigorous standardization of roughness in tornadic flow and pressure deficit dominated TLV flows led to high uncertainty in the results. More research needs to be accomplished for better characterization of surface roughness in tornado simulators.

The state-of-the-art tornado simulator, the WindEEE dome, is capable of producing a wide range of swirl ratios of TLVs utilizing their 4.5 m updraft diameter and around 4 m height (Hangan 2014; Hangan *et al.* 2017a, 2017b). This large-scale simulator can provide high spatial resolution for near-ground measurements. It is considered one of the best performing simulators as it accounts for geometric similarity based on multiple length scales as well as dynamic similarity represented by the high Reynolds number (Baker and Sterling, 2019). Therefore, ground surface and structural loadings can be explored adequately.

In this study, ground pressures analysis for stationary as well as translating TLVs was carried out over a wide range of swirl ratios (S=0.21 to S=1.03). The choice of the surface pressures as a characterizing tool is motivated by the following reasons: (i) the characterization of the velocity fields in the surface layer of TLVs is difficult to achieve even for stationary tornadoes, (Refan and Hangan, 2018); (ii) the surface pressure data is used to determine the effects of translation, roughness and swirl ratio on important TLV characteristics such as wandering, tilting and veering; (iii) the TLVs base pressure data is an important component that can be employed in the future for modeling tornado-induced pressures on buildings and structures based on the separation of the induced pressures between aerodynamic and tornado base pressure effects as put forward by Kikitsu and Okuda (2016) and discussed by Razavi and Sarkar (2018). The effect of variation of tornado translational speed reaching up to 1.5 m/s, (or $v_T/v_{tang,max} \leq 0.2$) for the first time in tornado simulators, was investigated in terms of ground pressure distributions, and TLV trajectories. Moreover, a preliminary study of surface roughness sequel on translating TLVs structure was performed. Finally, the effects of both translation speed and roughness on tornado tilting, veering, and wandering have been examined for the first time.

2. Experimental setup

2.1. Tornado simulator description

The WindEEE dome is a novel three-dimensional wind testing chamber which can simulate a wide variety of atmospheric flows such as atmospheric boundary layer (ABL), gust fronts, separated flows, thunderstorm downbursts, and tornadoes in a large-scale (4.5 m max. updraft diameter and 4 m height) and high Reynolds numbers (up to 2 × 106) (Hangan 2014; Hangan *et al.* 2017a; 2017b).

The test chamber has a hexagonal footprint with a diameter of 25 m. It is composed of 106 fans in total, 100 fans distributed along the circumference of the testing chamber, and the rest of the fans are positioned in the upper plenum above the test chamber (Fig. 1). The integration between the upper fans and the periphery fans doubled by an advanced control system sets the basis to produce a variety of flow-fields. Active control of the floor allows 1600 floor roughness elements to vary their heights between 0 and 30 cm to mimic different terrain exposures. Tornadoes can be simulated at WindEEE dome for a broad range of intensities out of which swirl ratios S=0.21 to 1.03 have been already explored. For the present experiments, mode "A" tornado was employed in which 6 fans in the upper plenum can produce the desired updraft in conjunction with a set of vanes situated at the base of the peripheral walls which when set at different angles can create the desired tornado swirl (see Fig. 1). The upper plenum is connected to the test chamber by a bell-mouth with mechanical louvers.

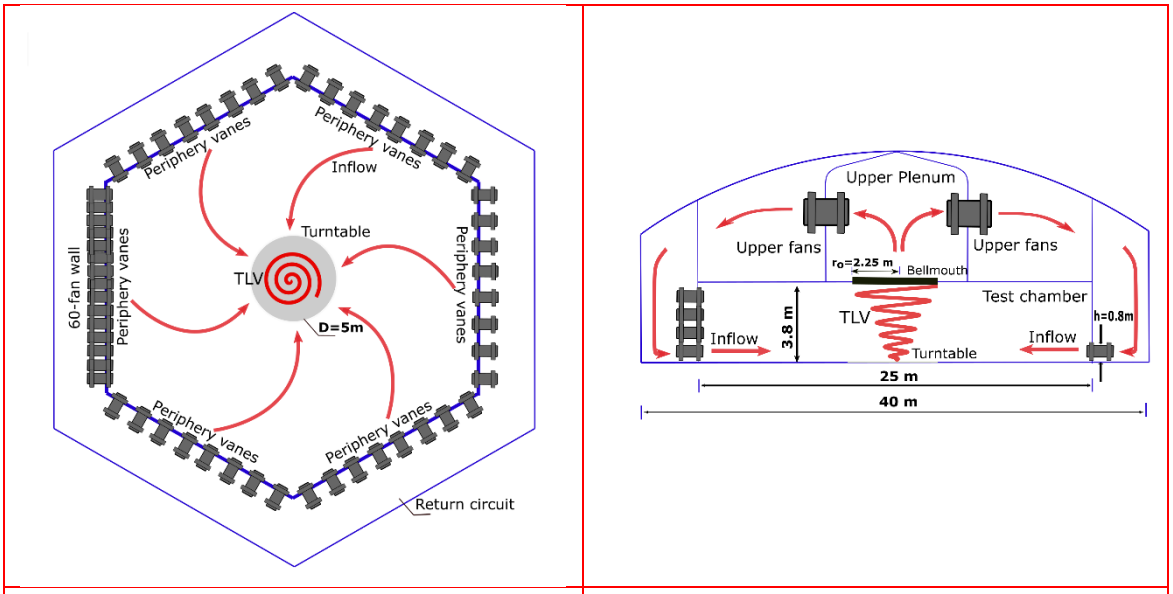

(a) (b)

Fig. 1 Schematic of tornado creation at WindEEE Dome (a) Plan view, and (b) Side view

An important feature of the simulator is its capability to produce translation. Simulated tornadoes can be translated over a 5 m distance and translation speeds up to 1.5 m/s. The 5 m translation path is equivalent to one-fifth of the chamber diameter. This is, to the authors' knowledge, the largest scale and translating speed in tornado simulators which can closely mimic the significant aerodynamic properties of tornadic flows (Baker and Sterling 2019). The translation mechanism utilizes a guillotine system, supported on two large beams, that translates the bell-mouth for up to 1.5 m/s utilizing a sophisticated control system, (Hangan 2014). The output voltage from the guillotine system is converted to a distance employing a conversion factor to track the guillotine movement. A flow visualization translating sequence is shown in Fig. 2 that demonstrates the movement of the surface vortex as well as the tilting of the vortex axis during translation. The same translation mechanism has been employed by (Kopp and Wu 2020). The simulator's large size also assures measurement resolution both in plan and in height which is very important for the characterization of tornado near-surface layer where most of the buildings and structures lie.

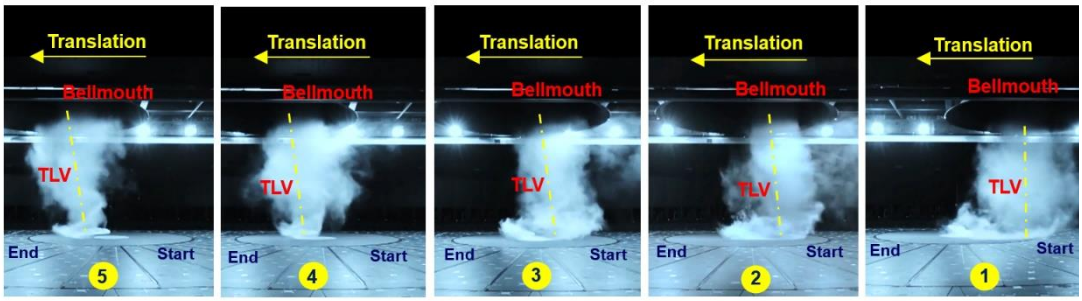

Fig. 2 Progressive shots of translating TLV movement at WindEEE Dome

2.2. Experimental setup and data processing

Tests were conducted at the WindEEE Dome. Detailed surface pressure measurements were carried out over a large area of the chamber floor (460 cm × 240 cm) to give a thorough insight into the tornado vortex dynamics near the ground where velocity measurements are difficult. TLVs were tested for swirl ratios between (S=0.21 to 1.03) and (S=0.48 and S=0.76) for stationary and translating TLV, respectively. Surface roughness was added utilizing the active control roughness blocks on the floor of a 3 cm mean height to examine the tornado flow-field characteristics.

Vortex flow-field:

The main parameters that control the tornado flow are: the geometric aspect ratio "a", the kinematic swirl ratio "S", and the dynamic radial Reynolds number "Re_r". The aspect ratio ($a = h/r_o$) is defined as the ratio between the inflow depth (h) and the updraft radius (r_o). The swirl ratio is defined as the ration between the angular momentum and the radial momentum which can be expressed as: $S = r_o\Gamma_{max}/2Qh$, where Γ_{max} is the maximum flow circulation and (Q) is the volumetric flow rate per unit axial length. The radial Reynolds number is expressed as: $Re_r = Q/2\pi\nu$, where ν is the kinematic viscosity of the fluid.

The swirl ratio in the test chamber can be controlled by altering the vanes' angles on the periphery walls. The flowrate is adjusted by regulating the top fans' rpm. For this set of experiments, the inflow depth was set at 0.8 m, the updraft radius was 2.25 m which resulted in an aspect ratio of 0.35 and the swirl ratios were 0.21, 0.48, 0.59, 0.76, 1.03. The geometric scale of the simulated TLV's are of the order of 1/150 to 1/280 (Refan and Hangan 2018). For more details on the flowrate measurement and swirl ratio calculations, see Refan and Hangan (2018).

Static pressure instrumentation:

A large rectangular base plate (460 mm × 240 mm), instrumented with 489 pressure taps, was employed in the present study, (see Fig. 3). The tap layout of the pressure plate was designed to ensure the full coverage of the whole travel distance of the translating tornado, with an adequate spatial resolution, particularly around the center of the tornado simulator, and to enclose larger width to account for translating tornado veering motion which was observed from flow visualizations as discussed later in the results section. This tap layout was determined to guarantee the accuracy of detecting the tornado trajectory path, specifically near the plate center, which is the region of interest, for future investigations of tornado loading on buildings. The pressure system consists of sixteen electronically scanned pressure (ESP) scanners and two digital temperature compensation (DTC) Initiums (Pressure Systems, Inc.), which were employed to accommodate the large number of pressure taps employed in the current study. The ESP scanners are minute electronic differential pressure units that incorporate a band of silicone piezoresistive pressure sensors, one for each pressure slot. Each ESP scanner can encompass up to 32 pressure ports and each port can accommodate PVC tubing with an outer diameter of 1 mm. The DTC initium system delivers a vigorous data acquisition system for the ESP scanners. Each Ethernet-based DTC initium can be hooked up to up-to 8 pressure scanners. For more information about the pressure system, see Refan and Hangan (2018).

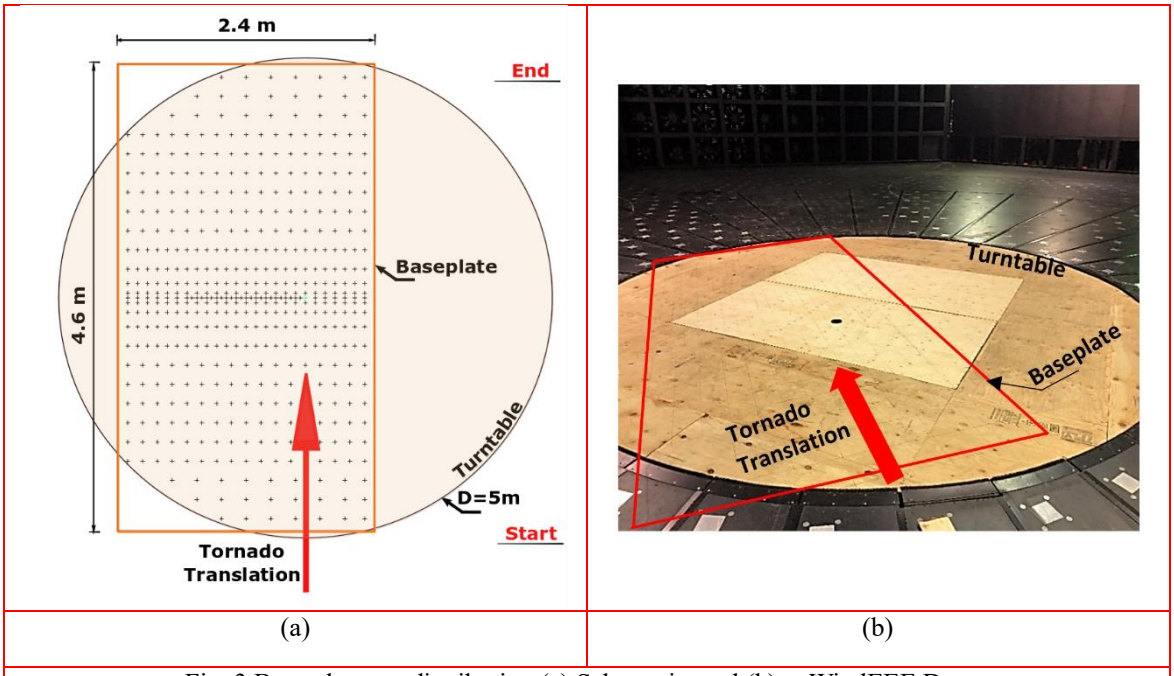

(a) (b)

Fig. 3 Base plate tap distribution (a) Schematic, and (b) at WindEEE Dome

To measure the pressure differential ($\Delta P = p_i - p_o$), where P_i is the ith tap static pressure, sensed by each pressure tap, the testing chamber' static pressure (p_o) was measured, outside the test chamber. Pressure measurements were acquired for five swirl ratios for stationary TLV, S =0.21, S =0.48, S =0.59, S =0.76, and S =1.03, and for S =0.48 and S =0.76 for translating TLV at Re_r =10^6. The selection of these two swirl ratios for translating TLV was attributed to simulating two important stages of TLV, the before and after touchdown of the tornado vortex (Refan and Hangan 2018). The sampling frequency and sampling time for the pressure measurements were 500 Hz and 40 s, respectively for translating tornado and 500 Hz and 16 s for stationary tornado. This high frequency was chosen to keep a good temporal resolution and the sampling time was long enough to cover the whole translating tornado movement.

Ground roughness:

The test chamber at WindEEE dome has 1600 pneumatically controlled roughness elements spread across the floor that can be extended to a maximum height of 30 cm. The automated roughness blocks are made from metal and are designed to accommodate a variety of exposure conditions for atmospheric boundary layer flows (ABL) and tornadic flow (Fig. 4). In the current study, a smooth surface and a rough surface were employed to preliminary investigate the effect of roughness on the tornado flow-field. For the first configuration, the roughness elements were not activated to reproduce flow over a smoothed surface in ABL flow-field. While the later was represented by active roughness elements of a mean height of 1.25 in as shown in Fig. 4. This configuration corresponds to open country (OC) terrain in ABL flow (aerodynamic roughness height, z_0 = 0.03 m) at 1:200 scale (Hangan *et al.* 2017). Although there is no standardization of roughness conditions in tornadic flow-field as the existing one in ABL flows, this study serves as a preliminary investigation of the roughness effect on translating TLVs structure.

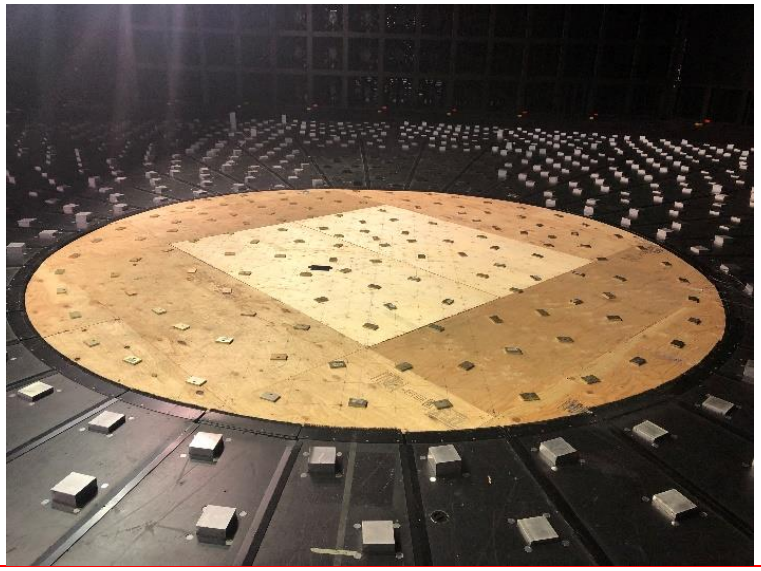

Fig. 4 Ground floor with added roughness elements in the test chamber at WindEEE Dome

3. Results and discussion

The tornado vortex structure near the ground is analyzed utilizing surface pressure measurements for a wide range of swirl ratios (S= 0.21, 0.48, 0.59, 0.76, and 1.03) for stationary and translating TLVs. Two translation speeds (0.11 m/s and 1.5 m/s) and two surface roughnesses of 0 cm (smooth) and 3 cm (rough), respectively were examined for translating TLV. The outcomes of the present study are motivated by (i) better understanding translating tornado TLVs effects such as wandering, tilting and veering under various translating and roughness conditions as well as (ii) providing detailed base pressure tornado data for future modeling of tornado-induced pressures on buildings and structures.

3.1. Stationary tornado

Fig. 5 shows the radial profiles of the normalized mean ground pressure deficits (ΔP^*) for several swirl ratios of stationary (non-translating) TLVs, where $\Delta P^*=\Delta P/0.5\ \rho\ v_{ax}^2$, where ρ is the density of air. The pressure was normalized employing the mean axial velocity "v_{ax}" measured at the bell-mouth location (Refan and Hangan, 2018). The mean axial velocity was chosen for normalization as it is uniform irrespective of the swirl ratio rather than the maximum tangential velocity which changes with swirl ratio. Hence, Using the maximum tangential velocity would provide misleading results regarding the pressure deficit comparison for the whole range of swirl ratios as (Refan and Hangan 2018). For the current study, the pressure data for each tap was averaged over the entire sampling duration of 16 s (8000 samples) without considering azimuthal averaging. This is because azimuthal averaging would be smoothing up the pressure deficit profile into a one-vortex structure regardless of the real vortex structure, one, two, or three-vortices.

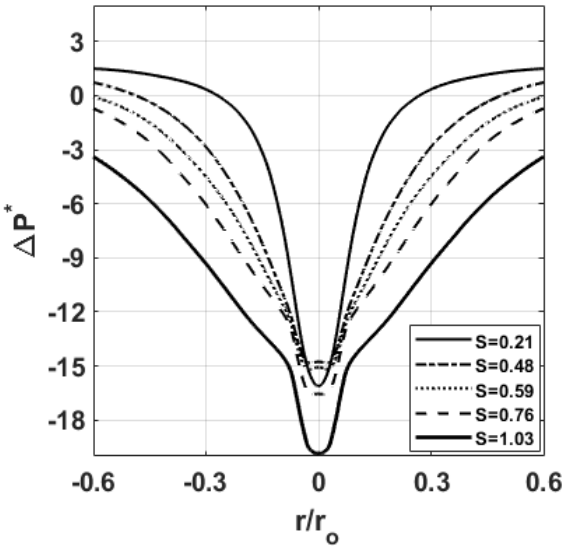

Fig. 5 mean surface pressure deficits for all swirl ratios. The pressure deficits are normalized based on $(0.5\rho v_{ax}^2)$

3.1.1 Wandering effects:

The pressure data shown in Fig. 5 represents the data after removing the effects of wandering. Wandering is a random oscillation of the vortex core departed from its real spatial position that would affect the resultant time-averaged data. The wandering behavior of TLVs influences the ground pressure profiles, particularly for low swirl ratios (e.g. Ashton *et al.* 2019; Refan and Hangan 2018).

In order to understand the extent of the tornado wandering behavior, the root mean square "rms" of the distance between the tornado instantaneous vortex center and the overall vortex center (i.e. the average vortex center over the whole sampling time) is quantified. Herein, the vortex center is determined by the detection of the minimum pressure at each instance. For the lowest swirl ratio, S=0.21, the high value of the rms 0.21 reflects the instability of the vortex at this supercritical stage before the touchdown of the vortex. Increasing the swirl ratio to S=0.48 resulted in a very slight decrease of the rms value to 0.2. Further increasing the swirl ratio resulted in a counterintuitive gradual increase (0.2- 0.3) in the rms value. This is attributed to the multiple sub-vortices intermittently present with increasing swirl ratio that makes detecting the vortex center challenging and adds error in the rms value. As a result, there is a need for a new method that can detect the vortex center rather than the minimum pressure which can be applicable for higher swirl ratios.

In order to obtain more precise results, the data should be corrected by removing wandering. Different approaches for eliminating wandering were implemented in previous studies: one approach is based on re-centering the vortex while another method uses a deconvolution procedure, but the foremost showed more accurate results as the second method resulted in an overestimation of the maximum tangential velocity in some cases (Ashton *et al.* 2019). Therefore, in this study, the first method of re-centering the vortex at each instance was initially adopted. Albeit the simplicity and efficiency of this approach in removing wandering for low swirl ratios, it did not provide

meaningful results for high swirls. This happened because the algorithm depends on determining the center of the tornado vortex based on the global minimum pressure recorded by the pressure taps, without accounting for the local minimums. This approach works well for only one-vortex structure while it fails for two or three-vortex structures that appear mostly at higher swirl ratios (S > 0.21). Hence, a new approach is proposed which proved to be more robust for this wide range of swirl ratios, particularly higher swirls. The adopted strategy was based on a moving average approach with proper window size. The algorithm used to eliminate wandering is outlined as follows:

1. Detection of the overall minimum pressure tap for each time step.
2. Plotting the moving average, with proper window size, of the radial pressure deficit.
3. Specifying the (X,Y) coordinates of the minimum of the moving average pressure profile.
4. Realigning the whole pressure flow-field, for each instance, to the center of the simulator (0,0) by the magnitude of (X,Y) shift.
5. Averaging the realigned pressure flow-field over the whole sampling time.

This method maintained the real shape of the pressure deficit, one-vortex or two-vortex, particularly for high swirl ratios, by accounting not only for the global minimum but also for the local minimums of the radial surface pressure profile which preserved the real shape of the vortex, either one-vortex or two-vortex. Wandering elimination resulted in a substantial difference in the minimum mean surface pressure magnitude, particularly for low swirl ratios as summarized in table (1). The results in Table 1 clearly show that not accounting for wandering would lead to a drastic underestimation of the pressure deficit.

Table 1 Effect of removing wandering on minimum mean surface pressure values of stationary tornado

Swirl Ratio (S)	ΔP^*_{min} **(Original data)**	ΔP^*_{min}**(removed wandering)**	**Error (%)**
0.21	-10.51	-16.11	-34.74
0.48	-13.06	-14.84	-11.95
0.59	-13.40	-15.19	-11.8
0.76	-13.64	-16.56	-17.62
1.03	-15.56	-19.85	-21.60

Fig. 6 shows the contour plot of the mean ground pressure for S=0.21 and S=1.03 before and after removing wandering. Table 1 and Fig. 6 show that wandering affects both the minimum pressure deficit value as well as its position. Note that the wandering effects are most important for low swirl where vortex instabilities are strong and at higher swirl where two and three sub-vortices are observed.

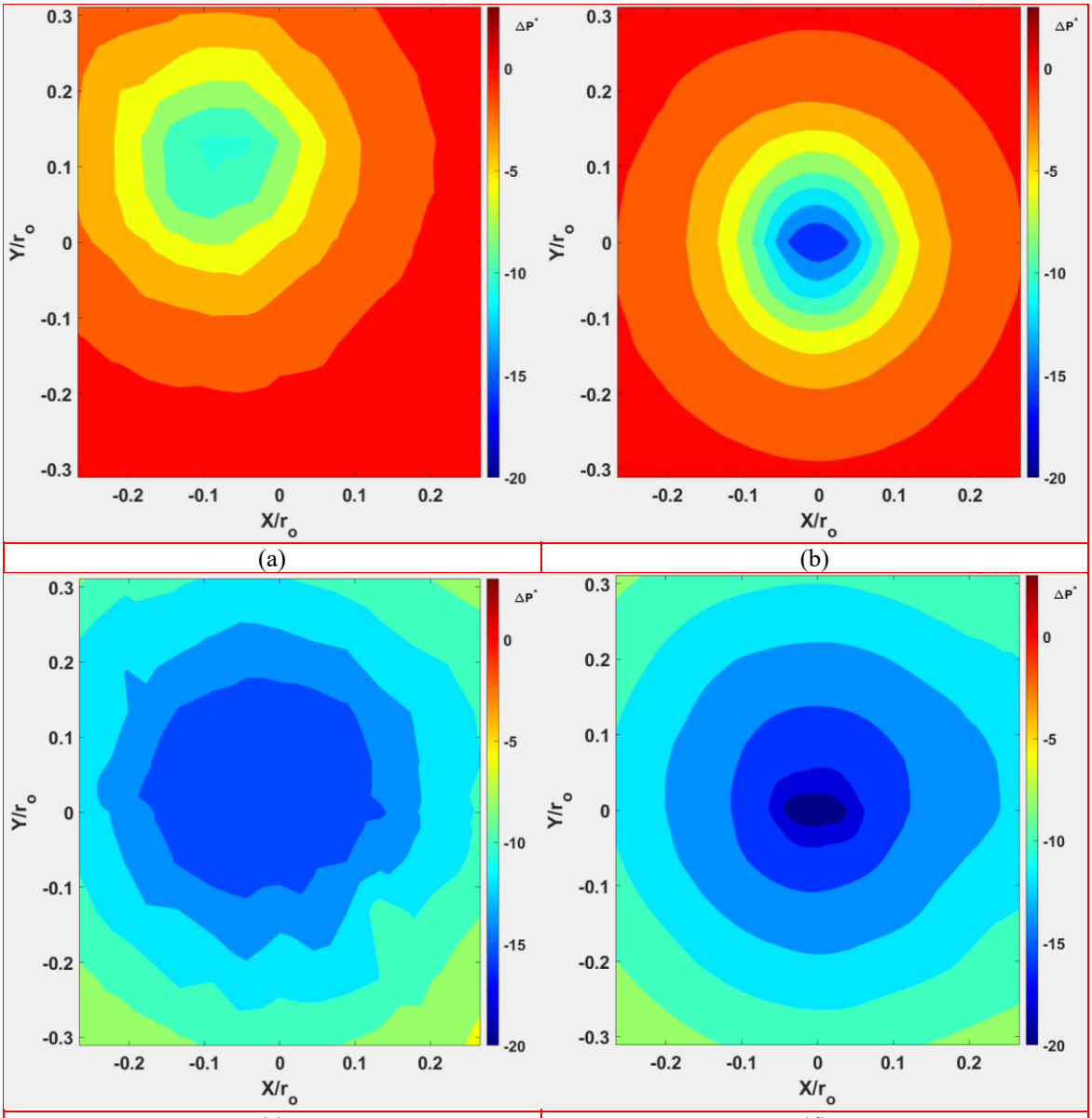

Fig. 6 Non-dimensional mean pressure deficit contour plot for S=0.21 and S=1.03 (a) with wandering (S=0.21), (b) after removing wandering (S=0.21), (c) with wandering (S=1.03), and (d) after removing wandering (S=1.03).

3.1.2 Swirl ratio effects:

Fig. 5 shows that for the lowest swirl ratio, S=0.21, the pressure deficit has a narrow profile, which indicates a smaller core radius compared to other swirl ratios, with a single minimum value characterizing a single-vortex TLV structure. An increase in the swirl ratio (S=0.48) decreased the suction and increased the core radius which led to a wider profile of the pressure deficit with a more

flattened peak possibly corresponding to a dual sub-vortex structure. The intermittent switch from one to two-vortex structure is associated with the vortex break down (VBD) and specifically to touchdown stage for swirl ratios here between S=0.48 and S=0.59 (Refan and Hangan 2018). Similar behavior was observed in previous studies (Snow *et al.* 1980; Refan and Hangan 2016; Tang *et al.* 2017). As the swirl ratio increases (S=0.76), the magnitude of the minimum pressure also increases where higher suctions are noticed, and a more pronounced two-vortex profile is observed. Moreover, the core radius keeps growing with increasing swirl. The pressure deficit was assumed to be symmetric, and Fig. 5 was plotted using half of the data. A comparison between the stationary and translating TLV is provided in the next section.

In order to better understand the tornado vortex dynamics near the ground, the vortex structure of the TLV was analyzed for two swirl ratios, S=0.76 and S=1.03 for a smooth surface and S=0.76 for a rough surface. Those two swirl ratios were chosen as they represent higher swirl ratios where the tornado vortex structure is more complex and tends to deviate from the classical single structure of the lower swirl ratio profiles. The detection of the vortices was based on the ground pressure contour plots utilizing image processing toolbox through MATLAB R2019b. Fig. 7 shows that the one-vortex structure is dominant with two-thirds of the probability of occurrence for S=0.76. The two-vortex follows with one third and the three-vortex which is less common with as low as 10% probability. Increasing the swirl ratio to 1.03 resulted in an increase in the two-vortex structure percentage to reach the same level as the one-vortex structure by almost 37%. Also, the three-vortex structure increases by 15% compared to S=0.76. This combination between two and three vortex-structure is a mark for high swirl ratios (Refan and Hangan 2018). On the other hand, adding roughness for S=0.76 led to an increase in the two and three vortex structure which may relate to the destabilizing of the main vortex by increased wall turbulence.

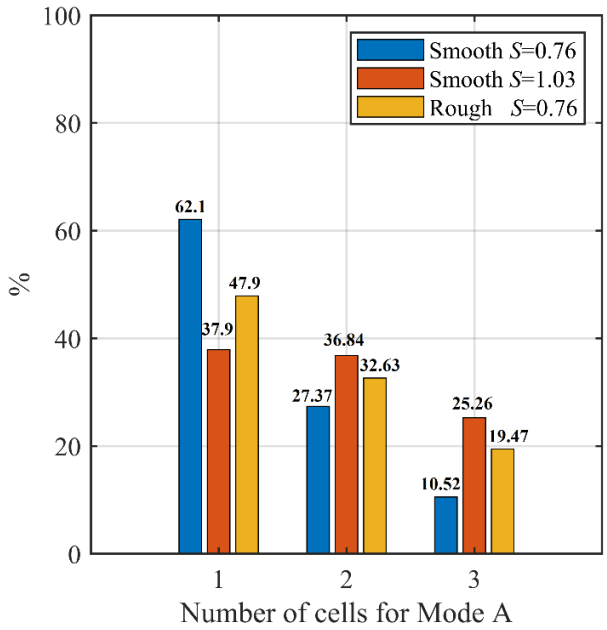

Fig. 7 Stationary TLV vortex structure

3.2 Translating tornado

In this section, pressure measurements on the ground are analyzed for translating TLV to examine the effects of swirl ratio, translation speed, and roughness. Comparison between stationary and translating TLVs is carried out to explore the important aspects that distinguish between the two cases.

3.2.1 Swirl ratio effects:

Fig. 8 shows the pressure deficit for simulated translating tornadoes in the WindEEE dome for two swirl ratios, S=0.48, and S=0.76. Those two swirl ratios are representative of EF-1 and EF-2 tornadoes (Refan and Hangan 2017), which are more frequent than the higher-rated (EF-3 to EF-5) tornadoes according to NOAA. They also represent before touchdown and after vortex touchdown patterns in TLVs. A translating speed of 1.5 m/s was used for this analysis. Each pressure deficit profile represents the timeseries of the minimum pressure tap along the centerline of the tornado simulator. For each case, ensemble averaging of five runs was performed. The number of runs was limited to accommodate the high number of test cases. Fig. 8 shows that the pressure deficit for both swirl ratios is distinctly asymmetric between the leading and the rear sides of the tornado vortex, unlike the stationary tornado which has a symmetric pressure profile., see Fig. 5. This observation is similar to field tornado observations (Lee and Samaras, 2004). Also, a wider profile of the pressure deficit due to the larger core radius is observed when the swirl ratio increases from 0.48 to 0.76. The pressure distribution for S=0.76 seems to present one minimum or at least one main minimum and a distorted one. This is different from stationary tornado studies (e.g. Tang *et al.*, 2017) and can be attributed to the higher translation speed in WindEEE ($V_{translating}$=1.5 m/s) that would result in a more inclined tornado vortex central axis.

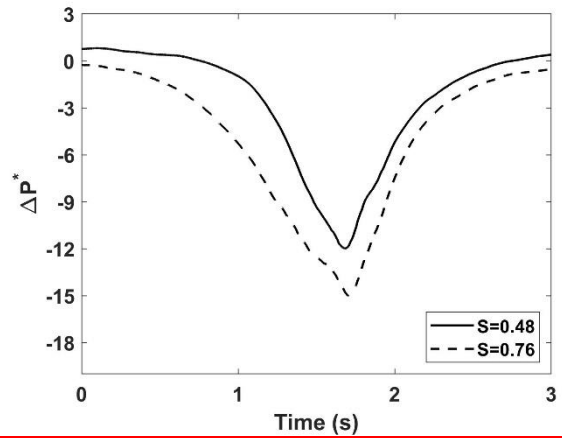

Fig. 8 Pressure deficit for S=0.48 and 0.76 for translating TLVs

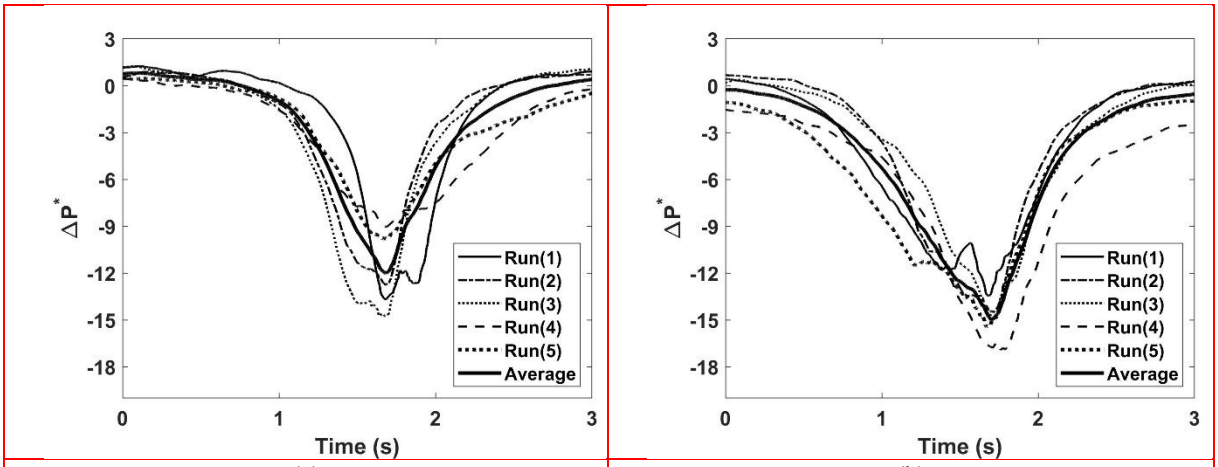

(a) (b)

Fig. 9 Effect of multiple runs on pressure deficit profile for (a) S=0.48 and (b) S=0.76

Fig. 9 represents the five runs for the two swirl ratios and the ensemble-averaged profile of the pressure deficit. It is clearly seen that ensemble averaging resulted in smoothing up the pressure deficit profiles and therefore making the two-vortex type profile (two minima) less pronounced for the two swirl ratios. This could be attributed to multiple factors. Firstly, the veering motion of the tornado, described in detail later in Section 3.2.5, may explain the variability in individual profiles for the five runs considered. Secondly, the surface friction increases with increasing swirl and produces a more pronounced asymmetry in the profiles for S=0.76 compared to S=0.48. This results in a forward inclination of the tornado central axis by less than 20° which was qualitatively observed in some full-scale data (Wurman and Gill 2000) as well as numerical simulations (e.g. Natarajan and Hangan 2012 and Liu and Ishihara 2016) and WindEEE flow visualizations. Lastly, the ensemble averaging process of the five runs was based on aligning the peak pressures which considers only the higher peak of the high swirl ratio cases.

In order to better understand the tornado vortex dynamics under translation, the analysis has been extended to a broader range of swirl ratios (Fig. 10), (S=0.21, 0.48, 0.59, 0.76, and 1.03). Note that due to the broader range of swirl ratios only one run was implemented and the alignment of the pressure profiles for the five swirl ratios was based on the peak pressures.

For S=0.21, it is apparent that the tornado is single-celled with a narrow profile and high peak pressure magnitude (Fig. 10). Amplifying the swirl ratio to S=0.48 caused an expansion of the core radius of the tornado vortex and an asymmetric vortex indicative of a two-cell profile. This asymmetry would be due to the higher translation speed of the tornado vortex that caused an inclination of the tornado axis as mentioned earlier. Also, a shift of the pressure deficit is observed due to aligning the pressure profiles based on the peak pressures. Further increasing the swirl ratio to S=0.59 led to a wider profile of the pressure deficit with multiple-vortex structure and a similar peak magnitude to S=0.48. Increasing the swirl ratio to S=0.76 resulted in a subsequent rise of the peak pressure and a broader core radius (i.e. wider pressure profile). The pressure deficit is multi-vortex and asymmetric. Further increasing the swirl ratio to S=1.03 led to very broad pressure deficit profile with a multi-vortex structure indicative of high swirl ratios.

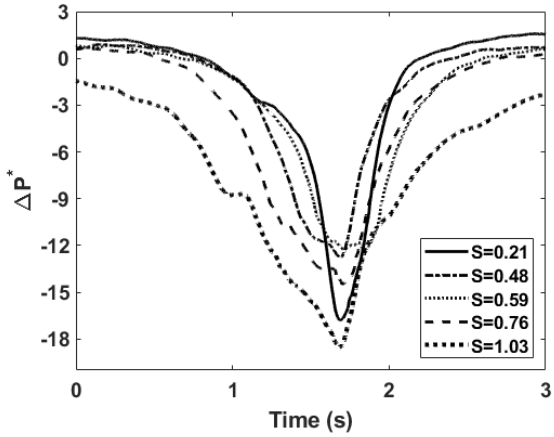

Fig. 10 Effect of increasing swirl ratio on the surface pressure deficit for translating TLVs

3.2.2 Translating vs. stationary tornado:

Comparison between the translating and the stationary tornado pressure deficit is provided for the ensembled averaged (5 runs) results only. For S=0.48 and S=0.76 (see Fig. 11), the translation resulted in a wider pressure deficit profile and a slight decrease in the magnitude of the minimum pressure deficit compared to stationary ones. Both of these effects are attributed to the increased surface shear due to translation. The widening of the pressure deficit profile is more pronounced for S=0.76 as the resultant velocity and therefore shear is larger for this case. Fig. 12 compares the minimum pressure values for stationary and translating TLVs (v_T =1.5 m/s). For stationary tornado, the maximum pressure deficit increases before vortex touchdown (S <0.48) and decreases after. This trend is comparable to previous studies for stationary tornadoes (Natarajan and Hangan 2012; Tang

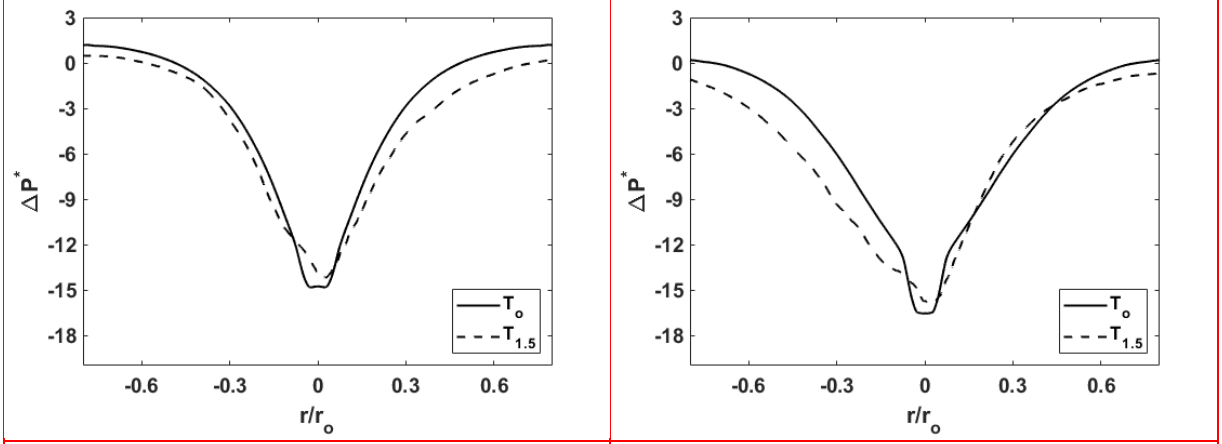

Fig. 11 Surface pressure deficit for Stationary (T_o) and Translating ($T_{1.5}$) TLVs for (a) S=0.48, and (b) S=0.76

et al. 2018). The trend seems to be the same for the translating cases ($T_{1.5}$) with a slight decrease in the negative peak magnitude due to additional surface shear. Note that the magnitude of the minimum pressure is dependent on the translation speed (i.e. the lower the translation speed, the lower the pressure loads) (Haan *et al.* 2011). This emphasizes the importance of proper representation of tornado translation speed and scaling to match field tornadoes.

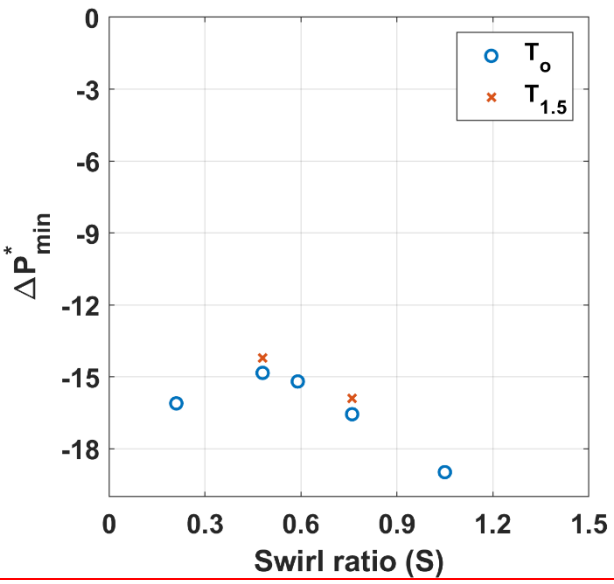

Fig. 12 Maximum central pressure deficit vs swirl ratio for stationary (T_o) and translating tornado ($T_{1.5}$)

3.2.3 Effect of translation speed:

The variation of tornado translating speed has a substantial effect on tornado loading patterns (e.g., Haan et al 2010). In this study, three different translating speeds, V_T =1.5 m/s "Speed (1)", 1 m/s "Speed (2)", and 0.11 "Speed (3)" were tested to analyze their effect on the tornado pressures on the ground surface. The higher speeds are closer to the lower end of observed field tornadoes and therefore they allow a more realistic representation of translating tornadoes and avoid overestimation of the loads.

Fig. 13a and Fig. 13b present pressure deficit radial profiles for the two swirl ratios considered and for several translational speeds. At lower translational speeds (2 and 3) the maximum pressure deficit is larger compared to the highest speed (1). Also, the pressure deficit profiles are more asymmetric for the lower speeds compared to the highest speed. This asymmetric behavior with multiple local minimums has been further investigated for S=0.48 and it was found that wandering is more pronounced when the translation velocity is low, particularly for low swirl ratios as this is considered a supercritical stage near the touchdown (Refan and Hangan 2018). Low translation speeds result in a higher drop in the pressure deficit which means overestimating the resultant loads. Hence, it is possible that using higher translation speeds closer to the scaled translation velocities in real tornadoes would produce more realistic and less conservative results.

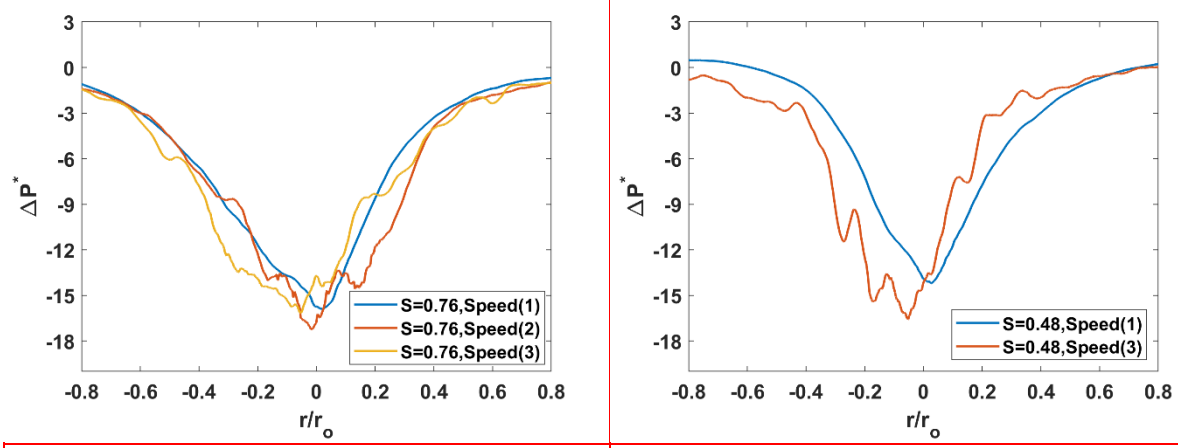

(a) (b)

Fig. 13 Effect of tornado translation speed on ground pressure (a) S=0.76, and (b) S=0.48

3.2.4 Effect of translation on tornado tilting

A prominent sighting from flow visualization was the vertical tilt of the tornado vortex axis towards the translation direction, specifically for the highest translating speed (Fig. 14a). The lower part of the vortex near the ground lagged behind the upper part causing a tilting of the tornado vortex axis. Fig. 14b shows a schematic sketch of the tilting behavior of the simulated tornado showing the inclination angle (θ). This inclination of the tornado axis will cause an asymmetric distribution of the velocity and consequently the surface pressures with implications on the overall aerodynamic loading on buildings. The inclination angle (θ) was deduced by employing the guillotine velocity (V_G), the tornado vortex base velocity (V_B), the total travel distance of the tornado ($D_T \cong$ 5 m), and the tornado vortex height (H=3.8 m) as follows:

$$\tan\theta = \frac{(D_T/2)(V_G/V_B - 1)}{H}$$

The tornado vortex base velocity (V_B) was calculated by tracing the signature of the tornado vortex on the ground utilizing the instantaneous minimum pressure tap. Besides, the guillotine velocity (V_G) was precisely estimated by converting the voltage sensed by the guillotine system to velocity using a voltage/meter conversion ratio. It was established that the tilt angle was ranging between 8 to 18 degrees for the whole range of swirl ratios. As mentioned before, this inclination of the tornado axis is attributed to higher shear stress with increasing velocity.

Similar behavior was recorded in previous experimental studies (Haan *et al.* 2010), however, no further investigation was performed. Also, the tilt in the tornado axis was calculated in a field study (Wurman and Gill 2000) as 20° and in some field and numerical studies (Brooks 1951; Brown et al 1978; Alexander and Wurman 2005; Liu and Ishihara 2016; Yuan *et al.* 2019).

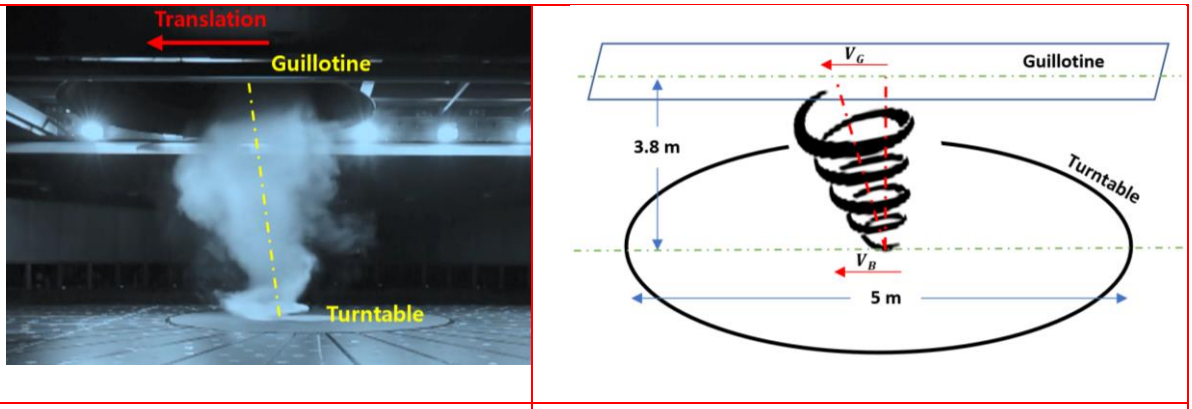

(a) (b)

Fig. 14 Tornado axis inclination (a) at WindEEE Dome, (b) Schematic Sketch

On the other hand, the tilting behavior of the TLV was examined for the lowest and highest translation speeds to understand its effect on the tornado vortex shape. For S=0.48 and S=0.76, the tilting angle for V_T =0.11 m/s "Speed (3)" was found to be almost zero degrees, unlike the highest speed V_T =1.5 m/s "Speed (1)" which resulted in a tilting angle in the range of 10° to 16°. This shows that, as expected, increasing the translation speed will result in a lagging behavior between the lower and upper parts of the tornado vortex.

3.2.5 Effects of translation speed on veering motion

Another important observation from the instantaneous contour plots of the translating tornado and the flow visualization is the veering motion of the vortex to the left of the translation direction. This veering behavior was observed mainly for the higher translation speeds for all swirl ratios. The real position of the tornado vortex near the surface was evaluated by tracking the minimum pressure tap at each instance (see Fig. 15b). It can be seen from the trajectories that at lower translating velocity, V_T =0.11 m/s "Speed (3)", the tornado approximately followed a straight path similar to the behavior of a low-intensity tornado observed by Baker (2020). Further increasing the translating speed resulted in a redirection of the tornado path on a curvature rather than a straight line to the left which is more pronounced in the highest translating velocity, V_T =1.5 m/s "Speed (1)". This effect is due to the asymmetry of the velocity field under translation and consequently the pressures between the right and left sides of the vortex. This phenomenon had not been reported in the literature before in tornado simulators, which may be related to the relatively low translation velocity in other simulators as the maximum achievable translating speed is 0.6 m/s (Haan *et al.* 2008). On the other hand, this deflection of the tornado path has been documented in field tornados by drawing the damage tracks of tornadoes (Lemon and Umscheid 2008) (see Fig. 15a). Wurman and Gill (2000) documented such behavior by comparing the tornado vortex signature on the lowest levels and on 1 km height which proved to be different as the highest levels showed almost a straight northward direction rather than a curved northwest direction of the lower portion of the tornado vortex on the ground.

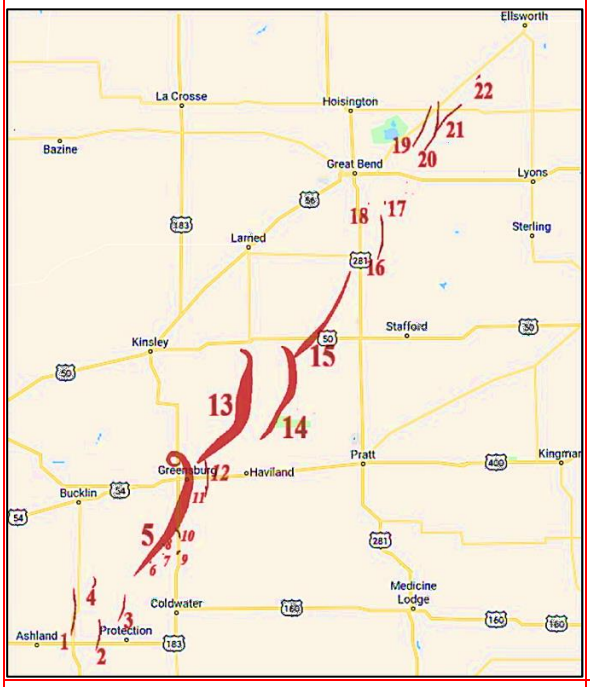

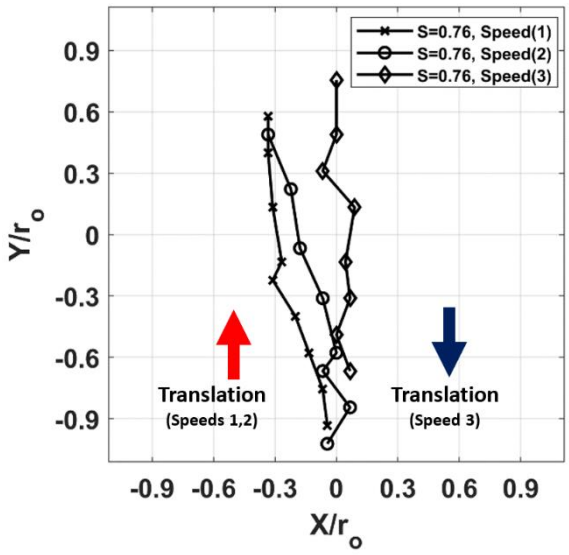

(a) (b)

Fig. 15 Tornado paths (a) Damage path of the Greensburg, KS tornado. Adapted from "The Greensburg, KS tornadic storm: a storm of extremes." by L. R. Lemon, & M. Umscheid, 2008, 24th Conf. on Severe Local Storms, 2.4. and (b) at WindEEE Dome

3.2.6 Effect of roughness

A preliminary investigation of roughness effects on TLVs was carried out by comparing the pressure deficit radial profiles for two surface roughness and two swirl ratios, S=0.48 and S=0.76. The heights of the 1,600 roughness blocks in the WindEEE Dome were set at 0 cm (smooth) and 3 cm (rough) average heights.

Fig. 16a compares the pressure deficit radial profiles for the two roughness levels and the two swirl ratios. For S =0.48, which is the stage just before VBD (Refan and Hangan 2018), introducing roughness resulted in a narrower pressure deficit profile, reduction in the core radius, and increase in the magnitude of the minimum pressure. This means that for low swirl ratios, roughness creates a similar effect as decreasing swirl ratio. This supports the previous studies' findings (Natarajan and Hangan 2012; Wang *et al.*, 2017). For S=0.76 (Fig. 16b), the same behavior was observed, and the roughness causes an analogous effect as the reduction of swirl ratio which is in agreement with previous studies' conclusions (e.g. Natarajan and Hangan, 2012, Razavi *et al.* 2018). More tests need to be performed to cover a wider range of swirl ratios and a larger set of roughness levels to obtain a full characterization of the overall effect of roughness with swirl ratio. The quantification of the surface layer relation to the roughness height through a roughness parameter analogous to the z_0 in ABL flows needs further consideration. On the other hand, the inclination angle of the tornado vortex axis was calculated similar to the smooth case and it was found that the tilt angle ranges between 9°

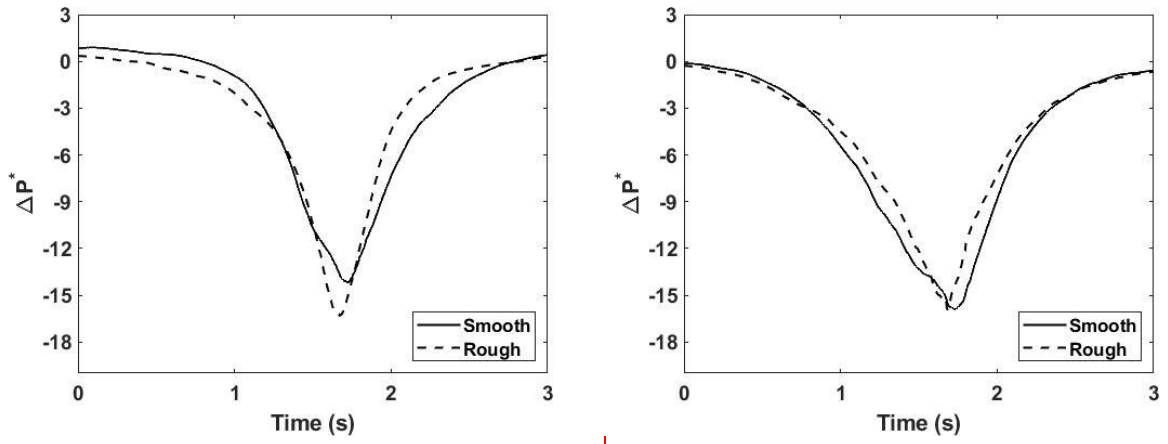

(a) (b)

Fig. 16 Effect of adding roughness to the ground on translating tornado surface loading (a) S=0.48, and (b) S=0.76

to 17° for both swirl ratios compared to 10° to 16° for smooth surface results. No obvious trend was noted for the relation between the inclination and the roughness level; however, the inclination was larger for the highest translation speed.

The effect of roughness on the TLV trajectory is captured in Fig. 17. There is a slight tendency that increased roughness decreases the veering of the TLV to the left for both Swirl ratios. This seems to be normal as increasing roughness translates in increased surface friction and lower surface translational speeds which overall diminishes the surface veering while, as shown above, slightly increases the tilting.

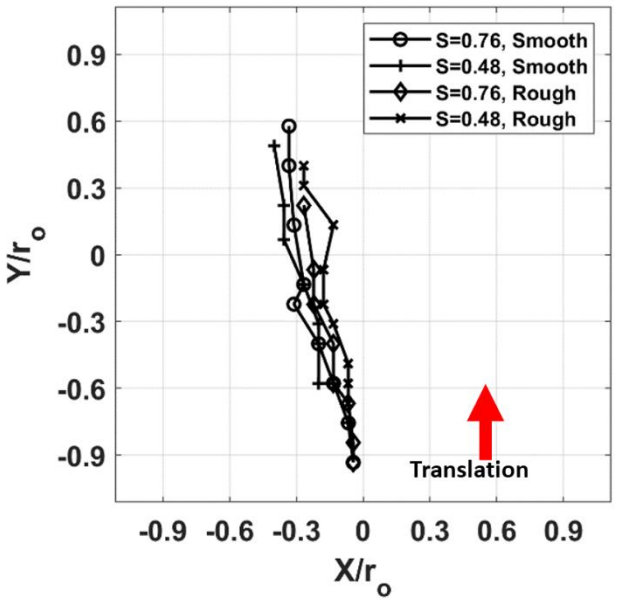

Fig. 17 Tornado trajectory for S=0.48 and S=0.76 for smooth and rough surfaces

4. Conclusions

Characteristics of stationary and translating TLVs are investigated in the state-of-the-art tornado simulator, the WindEEE Dome at Western University. High spatial and temporal resolution ground pressure measurements are performed to reveal the dynamics of stationary and translating TLVs as a function of swirl ratio, translation speeds, and roughness. The effects of these parameters on wandering, tilting, and veering of tornado vortices are for the first time examined.

Results indicate that the wandering behavior of the vortex has a substantial impact on stationary tornado mean flow-field, particularly for low swirl ratios. Wandering can lead to erroneous magnitudes of the minimum pressure deficit as high as 35%. A new method to eliminate wandering is proposed by using moving average to detect the center of the tornado deficit profile. This method proved to be more reliable specifically for higher swirl ratios compared to previous methods using re-centering the pressure deficit using the global minimum (e.g. Ashton *et al.* 2019).

For stationary tornadoes, the swirl ratio causes a reduction in the minimum pressure deficit magnitude followed by a subsequent increase. This highlights the different behavior of TLVs before and after the touchdown stage and the transition from one-vortex to a multi-vortex structure.

Translation speed effects on the TLVs are for the first time investigated over a range of speeds for 0.1 m/s; 1m/s and 1.5 m/s. It was observed that the maximum pressure deficit decreases with increasing translation speed. This implies that using stationary or low-speed tornado translation speeds for loading purposes may lead to overestimations.

One of the significant observations from the present study is the tilting of the translating tornado vortex due to increasing surface shear under translation. This tilt is significantly more pronounced for the highest translation speeds (i.e. V_T =1 m/s and 1.5 m/s) compared to the lowest speed (i.e. V_T =0.1 m/s). This tilting behavior has been reported in field tornadoes as well.

The veering motion of the tornado vortex to the left of the translation direction is also observed for higher translation speeds. This behavior is attributed to the asymmetry in the velocity field resulting from translation and is observed in full-scale tornadoes as well.

The effect of increased roughness has a similar effect to decreasing swirl ratio for the two studied cases (S=0.48 and S=0.76). Increased roughness also results in an increase in tilting and a decrease in veering of the TLV.

The surface pressure database created in this study is used to explore wandering, translation tilting, veering, and roughness effects in TLVs. The same data can provide a basis for interpretation and possible codification of tornado-induced pressures and loads on buildings as a superposition of pressure deficit and aerodynamic effects.

In the future, this study can be extended to a larger range of swirl ratios, and mostly to better understand the effects of surface roughness in tornado-like vortex flows.

Acknowledgments

This research has been made possible through funding from Natural Sciences and Engineering Research Council of Canada (NSERC) Discovery Grant (Grant number: R2811A03) and Canada Foundation for Innovation (CFI) WindEEE Dome Grant (Grant number: X2281838).

References

Alexander, C. R., & Wurman, J. (2005), "The 30 May 1998 Spencer, South Dakota, storm. Part I: The structural evolution and environment of the tornadoes", *Monthly Weather Review*, **133**(1), 72–96. https://doi.org/10.1175/MWR-2855.1

ASCE/SEI (ASCE/Structural Engineering Institute) (2016), "Minimum design loads for buildings and other structures", ASCE/SEI 7-16, Reston, VA

Ashton, R., Refan, M., Iungo, G. V., & Hangan, H. (2019), "Wandering corrections from PIV measurements of tornado-like vortices", Journal of Wind Engineering and Industrial Aerodynamics, **189**, 163-172. https://doi.org/10.1016/j.jweia.2019.02.010

Baker, C., & Sterling, M. (2019), "Are Tornado Vortex Generators fit for purpose?", Journal of Wind Engineering and Industrial Aerodynamics, **190**, 287-292. https://doi.org/10.1016/j.jweia.2019.05.011

Baker, G. L., & Church, C. R. (1979), "Measurements of core radii and peak velocities in modeled atmospheric vortices", Journal of Atmospheric Sciences, **36**(12), 2413-2424. https://doi.org/10.1175/1520-0469(1979)036<2413:mocrap>2.0.co;2

Bluestein, H. B., Weiss, C. C., & Pazmany, A. L. (2004), "The vertical structure of a tornado near Happy, Texas, on 5 May 2002: High-resolution, mobile, W-band, doppler radar observations", *Monthly Weather Review*, ***132***(10), 2325–2337. https://doi.org/10.1175/1520-0493(2004)132<2325:TVSOAT>2.0.CO;2

Brooks, E. M. (1951), "Tornadoes and related phenomena", In Compendium of Meteorology (pp. 673-680). American Meteorological Society, Boston, MA. https://doi.org/10.1007/978-1-940033-70-9_55

Brown, R. A., Lemon, L. R., & Burgess, D. W. (1978), "Tornado detection by pulsed Doppler radar", Monthly Weather Review, **106**(1), 29-38. https://doi.org/10.1175/1520-0493(1978)106<0029:TDBPDR>2.0.CO;2

Case, J., Sarkar, P., & Sritharan, S. (2014), "Effect of low-rise building geometry on tornado-induced loads", Journal of Wind Engineering and Industrial Aerodynamics, ***133***, 124–134. https://doi.org/10.1016/j.jweia.2014.02.001

Church, C., Snow, J. T., Baker, G. L., & Agee, E. M. (1979), "Characteristics of tornado-like vortices as a function of swirl ratio: A laboratory investigation", *Journal of Atmospheric Sciences*, ***36***(9), 1755-1776. https://doi.org/10.1175/1520-0469(1979)036<1755:COTLVA>2.0.CO;2

Dessens J. Jr. (1972), "Influence of ground roughness on tornadoes: a laboratory simulation", Journal of Applied Meteorology **11**(1):72–75. https://doi.org/10.1175/1520-0450(1972)0112.0.CO;2

Diamond, C. J., & Wilkins, E. M. (1984), "Translation effects on simulated tornadoes", Journal of the atmospheric sciences, **41**(17), 2574-2580. https://doi.org/10.1175/1520-0469(1984)041<2574:TEOST>2.0.CO;2

Fiedler, B. H., & Rotunno, R. (1986), "A theory for the maximum windspeeds in tornado-like vortices", *Journal of Atmospheric Sciences*, ***43***(21), 2328-2340. https://doi.org/10.1175/1520-0469(1986)043<2328:ATOTMW>2.0.CO;2

Fleming, M. R., Haan, F. L., & Sarkar, P. P. (2013), "Turbulent structure of tornado boundary layers with

translation and surface roughness", In *12th Americas Conf. on Wind Engineering (Seattle, WA)*.

Fujita, T. T. (1958), "Tornado cyclone: Bearing system of tornadoes", In *Proc. Seventh Conf. on Radar Meteorology* (pp. 1520-0493).

Gairola, A., & Bitsuamlak, G. (2019), "Numerical tornado modeling for common interpretation of experimental simulators", Journal of Wind Engineering and Industrial Aerodynamics, **186**, 32-48. https://doi.org/10.1016/j.jweia.2018.12.013

Geetha Rajasekharan, S., Matsui, M., & Tamura, Y. (2013), "Characteristics of internal pressures and net local roof wind forces on a building exposed to a tornado-like vortex", *Journal of Wind Engineering and Industrial Aerodynamics*, ***112***, 52–57. https://doi.org/10.1016/j.jweia.2012.11.005

Haan Jr, F. L., Balaramudu, V. K., & Sarkar, P. P. (2010), "Tornado-induced wind loads on a low-rise building", Journal of structural engineering, **136**(1), 106-116. https://doi.org/10.1061/(ASCE)ST.1943-541X.0000093

Haan Jr, F. L., Sarkar, P. P., & Gallus, W. A. (2008), "Design, construction and performance of a large tornado simulator for wind engineering applications", Engineering Structures, **30**(4), 1146-1159. https://doi.org/10.1016/j.engstruct.2007.07.010

Hangan, H. (2014), "The wind engineering energy and environment (WindEEE) dome at western university, Canada", Wind Engineers, JAWE, **39**(4), 350-351. https://doi.org/10.5359/jawe.39.350

Hangan, H., Refan, M., Jubayer, C., Parvu, D., & Kilpatrick, R. (2017), "Big data from big experiments. The WindEEE dome", In Whither Turbulence and Big Data in the 21st Century? (pp. 215-230). Springer, Cham. https://doi.org/10.1007/978-3-319-41217-7_12

Hangan, H., Refan, M., Jubayer, C., Romanic, D., Parvu, D., LoTufo, J., & Costache, A. (2017), "Novel techniques in wind engineering", Journal of Wind Engineering and Industrial Aerodynamics, **171**, 12-33. https://doi.org/10.1016/j.jweia.2017.09.010

Hu, H., Yang, Z., Sarkar, P., & Haan, F. (2011), "Characterization of the wind loads and flow fields around a gable-roof building model in tornado-like winds", *Experiments in Fluids*, ***51***(3), 835–851. https://doi.org/10.1007/s00348-011-1102-6

Ishihara, T., Oh, S., & Tokuyama, Y. (2011), "Numerical study on flow fields of tornado-like vortices using the LES turbulence model", Journal of wind engineering and industrial aerodynamics, **99**(4), 239-248. https://doi.org/10.1016/j.jweia.2011.01.014

Karami, M., Hangan, H., Carassale, L., & Peerhossaini, H. (2019), "Coherent structures in tornado-like vortices", Physics of Fluids, **31**(8), 085118. https://doi.org/10.1063/1.5111530

Karstens, C. D., Samaras, T. M., Lee, B. D., Gallus Jr, W. A., & Finley, C. A. (2010), "Near-ground pressure and wind measurements in tornadoes", Monthly Weather Review, **138**(7), 2570-2588. https://doi.org/10.1175/2010MWR3201.1

Kikitsu, H., & Okuda, Y. (2016), "Tornado-induced wind load model on a building considering relative size of building and tornado-like vortex", In Proc., 6th US-Japan Workshop on Wind Engineering (pp. 12-14).

Kopp, G. A., & Wu, C. H. (2020), "A framework to compare wind loads on low-rise buildings in tornadoes and atmospheric boundary layers", Journal of Wind Engineering and Industrial Aerodynamics, **204**, 104269.

https://doi.org/10.1016/j.jweia.2020.104269

Lee, J. J., Samaras, T., & Young, C. R. (2004, October), "Pressure measurements at the ground in an F-4 tornado", In Preprints, 22d Conf. on Severe Local Storms, Hyannis, MA, Amer. Meteor. Soc., 15.3.

Lee, W. C., & Wurman, J. (2005), "Diagnosed three-dimensional axisymmetric structure of the Mulhall tornado on 3 May 1999", Journal of the atmospheric sciences, **62**(7), 2373-2393. https://doi.org/10.1175/JAS3489.1

Lemon, L. R., & Umscheid, M. (2008), "The Greensburg, KS tornadic storm: a storm of extremes", 24th Conf. on Severe Local Storms, 2.4. http://ams.confex.com/ams/24SLS/techprogram/paper_141811.htm

Leslie, F. W. (1977), "Surface roughness effects on suction vortex formation: A laboratory simulation", Journal of the Atmospheric Sciences, **34**(7), 1022-1027. https://doi.org/10.1175/1520-0469(1977)034<1022:SREOSV>2.0.CO;2

Lewellen, W. S., Lewellen, D. C., & Sykes, R. I. (1997), "Large-eddy simulation of a tornado's interaction with the surface", Journal of the atmospheric sciences, **54**(5), 581-605. https://doi.org/10.1175/1520-0469(1997)054<0581:LESOAT>2.0.CO;2

Liu, Z., & Ishihara, T. (2015), "Numerical study of turbulent flow fields and the similarity of tornado vortices using large-eddy simulations", Journal of Wind Engineering and Industrial Aerodynamics, **145**, 42-60. https://doi.org/10.1016/j.jweia.2015.05.008

Liu, Z., & Ishihara, T. (2016), "Study of the effects of translation and roughness on tornado-like vortices by large-eddy simulations", Journal of Wind Engineering and Industrial Aerodynamics, **151**, 1-24. https://doi.org/10.1016/j.jweia.2016.01.006

Lombardo, F. T., Roueche, D. B., & Prevatt, D. O. (2015), "Comparison of two methods of near-surface wind speed estimation in the 22 May, 2011 Joplin, Missouri Tornado", Journal of Wind Engineering and Industrial Aerodynamics, **138**, 87-97. https://doi.org/10.1016/j.jweia.2014.12.007

Matsui, M., & Tamura, Y. (2009), "Influence of incident flow conditions on generation of tornado-like flow", In Proceedings of the 11th American Conference on Wind Engineering, Puerto Rico, USA.

Mishra, A. R., James, D. L., & Letchford, C. W. (2008), "Physical simulation of a single-celled tornado-like vortex, Part B: Wind loading on a cubical model", Journal of Wind Engineering and Industrial Aerodynamics, **96**(8-9), 1258-1273. https://doi.org/10.1016/j.jweia.2008.02.027

Nasir, Z., & Bitsuamlak, G. T. (2016), "NDM-557: COMPUTATIONAL MODELING OF HILL EFFECTS ON TORNADO LIKE VORTEX"

Natarajan, D., & Hangan, H. (2012), "Large eddy simulations of translation and surface roughness effects on tornado-like vortices", Journal of Wind Engineering and Industrial Aerodynamics, **104**, 577-584. https://doi.org/10.1016/j.jweia.2012.05.004

National Research Council of Canada. (2015), "National Building Code of Canada, 2015", National Research Council Canada.

National Weather Service. (2011), "NWS Central Region Service Assessment Joplin, Missouri, Tornado – May 22, 2011".

NOAA National Centers for Environmental Information, State of the Climate: Tornadoes for Annual 2011, published online January 2012, retrieved on January 20, 2020 from https://www.ncdc.noaa.gov/sotc/tornadoes/201113.

Nolan, D. S. (2005), "A new scaling for tornado-like vortices", Journal of the atmospheric sciences, **62**(7), 2639-2645. https://doi.org/10.1175/JAS3461.1

Nolan, D. S., & Farrell, B. F. (1999), "The structure and dynamics of tornado-like vortices", Journal of the Atmospheric Sciences, **56**(16), 2908-2936. https://doi.org/10.1175/1520-0469(1999)056<2908:TSADOT>2.0.CO;2

Nolan, D. S., Dahl, N. A., Bryan, G. H., & Rotunno, R. (2017), "Tornado vortex structure, intensity, and surface wind gusts in large-eddy simulations with fully developed turbulence", Journal of the Atmospheric Sciences, **74**(5), 1573-1597. https://doi.org/10.1175/JAS-D-16-0258.1

Razavi, A., & Sarkar, P. P. (2018), "Tornado-induced wind loads on a low-rise building: Influence of swirl ratio, translation speed and building parameters", Engineering Structures, **167**, 1-12. https://doi.org/10.1016/j.engstruct.2018.03.020

Razavi, A., Zhang, W., & Sarkar, P. P. (2018), "Effects of ground roughness on near-surface flow field of a tornado-like vortex", Experiments in Fluids, **59**(11), 1-16. https://doi.org/10.1007/s00348-018-2625-x

Refan, M., & Hangan, H. (2018), "Near surface experimental exploration of tornado vortices", Journal of Wind Engineering and Industrial Aerodynamics, **175**, 120-135. https://doi.org/10.1016/j.jweia.2018.01.042

Refan, M., Hangan, H., & Wurman, J. (2014), "Reproducing tornadoes in laboratory using proper scaling", Journal of Wind Engineering and Industrial Aerodynamics, **135**, 136-148. https://doi.org/10.1016/j.jweia.2014.10.008

Rhee, D. M., & Lombardo, F. T. (2018), "Improved near-surface wind speed characterization using damage patterns", Journal of Wind Engineering and Industrial Aerodynamics, **180**, 288-297. https://doi.org/10.1016/j.jweia.2018.07.017

Sengupta, A., Haan, F. L., Sarkar, P. P., & Balaramudu, V. (2006), "Transient loads on buildings in microburst and tornado winds", In Proc. The fourth International Symposium on Comp. Wind Engr.(CWE2006).

Sengupta, A., Haan, F. L., Sarkar, P. P., & Balaramudu, V. (2008), "Transient loads on buildings in microburst and tornado winds", Journal of Wind Engineering and Industrial Aerodynamics, **96**(10-11), 2173-2187. https://doi.org/10.1016/j.jweia.2008.02.050

Snow, J. T. (1982), "A review of recent advances in tornado vortex dynamics", Reviews of Geophysics, **20**(4), 953-964. https://doi.org/10.1029/RG020i004p00953

Snow, J. T., & Lund, D. E. (1997), "Considerations in exploring laboratory tornadolike vortices with a laser Doppler velocimeter", Journal of Atmospheric and Oceanic Technology, **14**(3), 412-426. https://doi.org/10.1175/1520-0426(1997)014<0412:CIELTV>2.0.CO;2

Snow, J. T., Church, C. R., & Barnhart, B. J. (1980), "An investigation of the surface pressure fields beneath simulated tornado cyclones", Journal of the Atmospheric Sciences, **37**(5), 1013-1026. https://doi.org/10.1175/1520-0469(1980)037<1013:AIOTSP>2.0.CO;2

Tang, Z., Feng, C., Wu, L., Zuo, D., & James, D. L. (2018), "Characteristics of tornado-like vortices simulated in a large-scale ward-type simulator", Boundary-layer meteorology, **166**(2), 327-350. https://doi.org/10.1007/s10546-017-0305-7

Tari, P. H., Gurka, R., & Hangan, H. (2010), "Experimental investigation of tornado-like vortex dynamics with swirl ratio: The mean and turbulent flow fields", Journal of Wind Engineering and Industrial Aerodynamics, **98**(12), 936-944. https://doi.org/10.1016/j.jweia.2010.10.001

Tepper, M., & Eggert, W. E. (1956), "Tornado proximity traces", Bulletin of the American Meteorological Society, **37**(4), 152-159. https://doi.org/10.1175/1520-0477-37.4.152

Thampi, H., Dayal, V., & Sarkar, P. P. (2011), "Finite element analysis of interaction of tornados with a low-rise timber building", Journal of Wind Engineering and Industrial Aerodynamics, ***99***(4), 369–377. https://doi.org/10.1016/j.jweia.2011.01.004

Wakimoto, R. M., Atkins, N. T., & Wurman, J. (2011), "The LaGrange tornado during VORTEX2. Part I: Photogrammetric analysis of the tornado combined with single-Doppler radar data", Monthly weather review, **139**(7), 2233-2258. https://doi.org/10.1175/2010MWR3568.1

Wakimoto, R. M., Murphey, H. V., Dowell, D. C., & Bluestein, H. B. (2003), "The Kellerville tornado during VORTEX: Damage survey and Doppler radar analyses", Monthly weather review, **131**(10), 2197-2221. https://doi.org/10.1175/1520-0493(2003)131<2197:TKTDVD>2.0.CO;2

Wakimoto, R. M., Stauffer, P., Lee, W. C., Atkins, N. T., & Wurman, J. (2012), "Finescale structure of the LaGrange, Wyoming, tornado during VORTEX2: GBVTD and photogrammetric analyses", Monthly weather review, **140**(11), 3397-3418. https://doi.org/10.1175/MWR-D-12-00036.1

Wang, J., Cao, S., Pang, W., & Cao, J. (2017), "Experimental study on effects of ground roughness on flow characteristics of tornado-like vortices", Boundary-Layer Meteorology, **162**(2), 319-339. https://doi.org/10.1007/s10546-016-0201-6

Wang, J., Cao, S., Pang, W., Cao, J., & Zhao, L. (2016), "Wind-load characteristics of a cooling tower exposed to a translating tornado-like vortex", Journal of Wind Engineering and Industrial Aerodynamics, **158**, 26-36. https://doi.org/10.1016/j.jweia.2016.09.008

Ward, N. B. (1972), "The exploration of certain features of tornado dynamics using a laboratory model", Journal of the Atmospheric Sciences, **29**(6), 1194-1204. https://doi.org/10.1175/1520-0469(1972)029<1194:TEOCFO>2.0.CO;2

Wurman, J. (2002), "The multiple-vortex structure of a tornado", Weather and forecasting, **17**(3), 473-505. https://doi.org/10.1175/1520-0434(2002)017<0473:TMVSOA>2.0.CO;2

Wurman, J., & Alexander, C. R. (2005), "The 30 May 1998 Spencer, South Dakota, storm. Part II: Comparison of observed damage and radar-derived winds in the tornadoes", Monthly weather review, **133**(1), 97-119. https://doi.org/10.1175/MWR-2856.1

Wurman, J., & Gill, S. (2000), "Finescale radar observations of the Dimmitt, Texas (2 June 1995), tornado", Monthly weather review, **128**(7), 2135-2164. https://doi.org/10.1175/1520-0493(2000)128<2135:FROOTD>2.0.CO;2

Wurman, J., & Samaras, T. (2004), "Comparison of in-situ pressure and DOW Doppler winds in a tornado and

RHI vertical slices through 4 tornadoes during 1996–2004", Preprints, 22nd Conf. on Severe Local Storms, Hyannis, MA, Amer. Meteor. Soc., 15.4. [Available online at http://ams.confex.com/ams /pdfpapers/82352.pdf.]

Wurman, J., Straka, J. M., & Rasmussen, E. N. (1996), "Fine-scale Doppler radar observations of tornadoes", Science, **272**(5269), 1774-1777. https://doi.org/10.1126/science.272.5269.1774

Wurman, J., Straka, J., Rasmussen, E., Randall, M., & Zahrai, A. (1997), "Design and deployment of a portable, pencil-beam, pulsed, 3-cm Doppler radar", Journal of Atmospheric and Oceanic Technology, **14**(6), 1502-1512. https://doi.org/10.1175/1520-0426(1997)014<1502:DADOAP>2.0.CO;2

Yuan, F., Yan, G., Honerkamp, R., Isaac, K. M., Zhao, M., & Mao, X. (2019), "Numerical simulation of laboratory tornado simulator that can produce translating tornado-like wind flow", Journal of Wind Engineering and Industrial Aerodynamics, **190**, 200-217. https://doi.org/10.1016/j.jweia.2019.05.001

Zhang, W., & Sarkar, P. P. (2008), "Effects of ground roughness on tornado like vortex using PIV", In Proceedings of the AAWE workshop, Vail, CO.

Zhang, W., & Sarkar, P. P. (2012), "Near-ground tornado-like vortex structure resolved by particle image velocimetry (PIV)", Experiments in fluids, **52**(2), 479-493. https://doi.org/10.1007/s00348-011-1229-5